NA49 RESULTS ON SINGLE PARTICLE AND CORRELATION MEASUREMENTS IN CENTRAL PB+PB COLLISIONS

F. WANG [a]
Lawrence Berkeley National Lab, Berkeley, CA 94720, USA
E-mail: FQWang@lbl.gov

for the NA49 Collaboration:
H. Appelshäuser[7,#], J. Bächler[5], S.J. Bailey[17], D. Barna[4], L.S. Barnby[3], J. Bartke[6], R.A. Barton[3], H. Białkowska[15], A. Billmeier[10], C.O. Blyth[3], R. Bock[7], B. Boimska[15], C. Bormann[10], F.P. Brady[8], R. Brockmann[7,†], R. Brun[5], P. Bunčić[5,10], H.L. Caines[3], L.D. Carr[17], D. Cebra[8], G.E. Cooper[2], J.G. Cramer[17], M. Cristinziani[13], P. Csato[4], J. Dunn[8], V. Eckardt[14], F. Eckhardt[13], M.I. Ferguson[5], H.G. Fischer[5], D. Flierl[10], Z. Fodor[4], P. Foka[10], P. Freund[14], V. Friese[13], M. Fuchs[10], F. Gabler[10], J. Gal[4], R. Ganz[14], M. Gaździcki[10], E. Gładysz[6], J. Grebieszkow[16], J. Günther[10], J.W. Harris[18], S. Hegyi[4], T. Henkel[13], L.A. Hill[3], H. Hümmler[10,+], G. Igo[12], D. Irmscher[7], P. Jacobs[2], P.G. Jones[3], K. Kadija[19,14], V.I. Kolesnikov[9], M. Kowalski[6], B. Lasiuk[12,18], P. Lévai[4] A.I. Malakhov[9], S. Margetis[11], C. Markert[7], G.L. Melkumov[9], A. Mock[14], J. Molnár[4], J.M. Nelson[3], M. Oldenburg[10], G. Odyniec[2], G. Palla[4], A.D. Panagiotou[1], A. Petridis[1], A. Piper[13], R.J. Porter[2], A.M. Poskanzer[2], D.J. Prindle[17], F. Pühlhofer[13], W. Rauch[14], J.G. Reid[17], R. Renfordt[10], W. Retyk[16], H.G. Ritter[2], D. Röhrich[10], C. Roland[7], G. Roland[10], H. Rudolph[10], A. Rybicki[6], A. Sandoval[7], H. Sann[7], A.Yu. Semenov[9], E. Schäfer[14], D. Schmischke[10], N. Schmitz[14], S. Schönfelder[14], P. Seyboth[14], J. Seyerlein[14], F. Sikler[4], E. Skrzypczak[16], R. Snellings[2], G.T.A. Squier[3], R. Stock[10], H. Ströbele[10], Chr. Struck[13], I. Szentpetery[4], J. Sziklai[4], M. Toy[2,12], T.A. Trainor[17], S. Trentalange[12], T. Ullrich[18], M. Vassiliou[1], G. Veres[4], G. Vesztergombi[4], S. Voloshin[2], D. Vranić[5,19], F. Wang[2], D.D. Weerasundara[17], S. Wenig[5], C. Whitten[12], T. Wienold[2,#], L. Wood[8], N. Xu[2], T.A. Yates[3], J. Zimanyi[4], X.-Z. Zhu[17], R. Zybert[3]

[1] *Department of Physics, University of Athens, Athens, Greece.*
[2] *Lawrence Berkeley National Laboratory, University of California, Berkeley, USA.*
[3] *Birmingham University, Birmingham, England.*
[4] *KFKI Research Institute for Particle and Nuclear Physics, Budapest, Hungary.*
[5] *CERN, Geneva, Switzerland.*
[6] *Institute of Nuclear Physics, Cracow, Poland.*
[7] *Gesellschaft für Schwerionenforschung (GSI), Darmstadt, Germany.*
[8] *University of California at Davis, Davis, USA.*
[9] *Joint Institute for Nuclear Research, Dubna, Russia.*

[a] Invited talk given at the XXVIII International Symposium on Multiparticle Dynamics, Delphi, Greece, September 6–11, 1998

[10] *Fachbereich Physik der Universität, Frankfurt, Germany.*
[11] *Kent State University, Kent, OH, USA.*
[12] *University of California at Los Angeles, Los Angeles, USA.*
[13] *Fachbereich Physik der Universität, Marburg, Germany.*
[14] *Max-Planck-Institut für Physik, Munich, Germany.*
[15] *Institute for Nuclear Studies, Warsaw, Poland.*
[16] *Institute for Experimental Physics, University of Warsaw, Warsaw, Poland.*
[17] *Nuclear Physics Laboratory, University of Washington, Seattle, WA, USA.*
[18] *Yale University, New Haven, CT, USA.*
[19] *Rudjer Boskovic Institute, Zagreb, Croatia.*
[†] *deceased.*
[#] *present address: Physikalisches Institut, Universitaet Heidelberg, Germany.*
[+] *present address: Max-Planck-Institut für Physik, Munich, Germany.*

Single-particle spectra and two-particle correlation functions measured by the NA49 collaboration in central Pb+Pb collisions at 158 GeV/nucleon are presented. These measurements are used to study the kinetic and chemical freeze-out conditions in heavy ion collisions. We conclude that large baryon stopping, high baryon density and strong transverse radial flow are achieved in central Pb+Pb collisions at the SPS.

1 Introduction

The goal of studying high energy heavy-ion collisions is to understand the properties of nuclear matter under extreme conditions of high energy density (> 1 GeV/fm^3). It is unlikely under such conditions that spatially separated hadrons exist. Instead, formation of quark-gluon-plasma (QGP), in which quarks and gluons are deconfined over an extended volume, is expected. [1,2,3,4] This state of matter might have existed in the early universe shortly after the Big Bang. [5]

If a QGP is produced in a heavy ion collision, the collision system will undergo transitions from hadrons (initial nucleons in the incoming nuclei), to partons, to interacting hadrons, to, finally, freeze-out particles where the measurements are realized. Many signatures of QGP formation have been proposed. [6] These include enhanced production of strangeness, [7] charm [8] and leptons, [9] jet quenching, [10] collective radial flow, [11] etc. However, none of the signatures is conclusive, and many can be produced by secondary particle interactions. [12,13] Therefore, systematic studies of multiple observables are necessary in the searching of the QGP formation in heavy ion collisions.

CERN SPS experiment NA49 has measured many observables of Pb+Pb collisions at 158 GeV/nucleon. These measurements include transverse energy production, [14] baryon stopping and negative hadron distributions, [15] negative hadron [16] and proton [17] two-particle correlation functions, and charged and

neutral strange particle distributions[18,19] in central collisions, and directed and elliptic flow in non-central collisions.[20] In this talk, only selected results from central Pb+Pb collisions are presented. Distributions of net baryons, negative hadrons, and charged kaons are presented in Sect. 2 to address the chemical freeze-out conditions. Negative hadron and proton two-particle correlation functions are presented in Sect. 3 to address the kinetic freeze-out conditions. Conclusions are drawn in Sect. 4. The results which have been published or have been submitted for publication are not duplicated here but are referred to. All the plots shown here are preliminary.

NA49 is a large acceptance hadron experiment,[21] measuring about 800 charged particles in a central Pb+Pb event. The experimental apparatus consists of four large time-projection chambers (TPCs). Two of them are placed along the beam axis inside two dipole magnets, which have maximum integrated field strength of 9 Tesla-meters. The other two are downstream of the magnets on either side of the beam axis. Further downstream are four time-of-flight (TOF) walls covering smaller acceptance than the TPCs. The particle identification was performed by measuring the specific ionization (dE/dx) deposited by charged particles in the TPCs,[22] and the velocities of the particles[23] in the TOF walls. The dE/dx resolution was 5%, and the TOF resolution was 60 ps. A beam of Pb nuclei struck on a Pb target of thickness 224 mg/cm^2 placed in front of the first TPC. A zero-degree hadronic calorimeter,[14,24] located downstream along the beam-axis, measured mainly the energy remnant in the projectile spectators. By applying a threshold on the measured energy as an experimental trigger, the 5% most central events were recorded. These events corresponded to collisions with impact parameter below 3.3 fm.

2 Single-particle distributions

Extensive studies of Si+A and Au+Au collisions at the BNL AGS and S+A collisions at the CERN SPS have shown that nucleus-nucleus collisions are not mere superpositions of nucleon-nucleon collisions (N+N) at the corresponding energies.[6] Protons are shifted further into the central rapidity region (baryon stopping) in these collisions[25,26,27,28] than in N+N[29]. The NA49 result on the net baryon rapidity distribution in central Pb+Pb collisions over a wide rapidity range (Fig.1 in Ref[15]) shows a larger average rapidity shift than that in S+S (3% centrality).[27,28] This is consistent with the picture of more multiple collisions suffered by each nucleon on average in Pb+Pb than in S+S.

A larger fraction of energy is converted from the longitudinal direction into the transverse direction in Pb+Pb central collisions than in S+S. Two consequences can be expected: more particle production and/or stronger transverse

expansion in Pb+Pb than S+S. Products from high energy heavy ion collisions are dominantly pions. The rapidity distribution of negative hadrons (h^-), mainly π^-'s, scales with number of participants from S+S to Pb+Pb central collisions almost perfectly (Fig.2 in Ref[15]), in contrast to the different net baryon distributions. Since the total pion multiplicity provides a good approximation to the total entropy produced, the scaling implies that no extra entropy per participant was generated in Pb+Pb central collisions with respect to S+S. However, one should note that pion production does not scale from N+N to S+S.[30] Collective transverse expansion is reflected in particle transverse distributions; heavy particles pick up more transverse momentum from the expansion than light particles, exhibiting larger inverse slopes of the exponential transverse mass ($m_\perp = \sqrt{p_\perp^2 + m^2}$) spectra. In Fig. 1, the inverse slopes are plotted against particle masses (m) for three systems: Pb+Pb [18] and S+S [31] at the SPS, and Au+Au at the AGS.[25,32] The inverse slope systematically increases with particle mass in all three systems, consistent with the picture of collective transverse radial flow. The inverse slope is larger in heavy system Pb+Pb than light system S+S at similar energies, and is larger at high energy (SPS) than low energy (AGS) in systems with similar sizes.

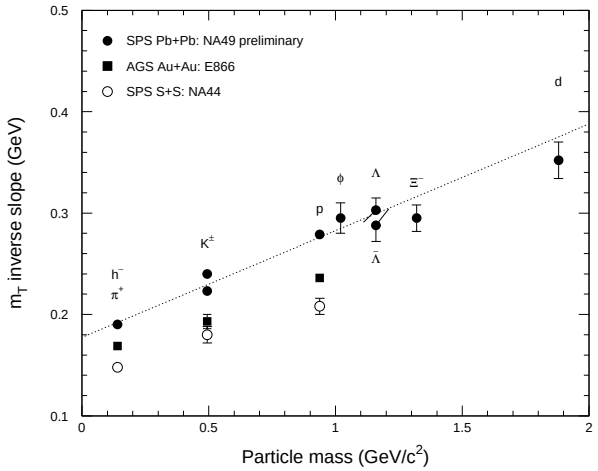

Figure 1: Mass systematics of inverse slopes of particle $m_\perp$ spectra in the central rapidity region for three central collision systems: Pb+Pb (5%) at $\sqrt{s}$ = 17.3 GeV, S+S (3%) at $\sqrt{s}$ = 19.4 GeV, and Au+Au (4%) at $\sqrt{s}$ = 4.74 GeV. The straight line is to guide the eye.

Kaons, carrying most of the strangeness produced in heavy ion collisions at SPS energy and lower, have been extensively studied. NA49 has measured charged kaon production at mid-rapidity by the TOF walls and over wide

rapidity range by the TPCs. The kaon $m_\perp$ spectra, can be well described by single exponential functions. At mid-rapidity, the inverse slopes are measured to be 240 ± 4 MeV for K^+ and 223 ± 3 MeV for K^-, and the yields per unit rapidity are estimated to be $dN/dy = 29.8 \pm 0.9$ (K^+) and 16.2 ± 0.5 (K^-).

The K^+/K^- ratio is sensitive to the baryon density. In Fig. 2, the ratio at mid-rapidity is plotted against the mid-rapidity ratio of net-baryon yield over total-multiplicity for Si+A [33,34,35] and Au+Au [25,36,37] central collisions at the AGS and S+S [26,27,38] and Pb+Pb [15] central collisions at the SPS. The total multiplicity at mid-rapidity is approximated by the sum of the net baryon yield and $3\langle\pi\rangle$ at mid-rapidity, where $\langle\pi\rangle = (\langle\pi^+\rangle + \langle\pi^-\rangle)/2$ for the AGS data and $\langle\pi\rangle = \langle h^-\rangle$ for the SPS data. Note that both the abscissa and the ordinate are experimentally measured quantities. However, the motivation to plot this way is that the ratio of net-baryon yield over total multiplicity is proportional to the average baryon density at freeze-out, assuming that the volume of the system scales with the total multiplicity. The K^+/K^- ratio in e^+e^- at LEP [39] is also plotted. As seen from the plot, the K^+/K^- ratio has strong dependence on the baryon density. Note that the baryon density in heavy ion collisions is higher at low energies and in large systems.

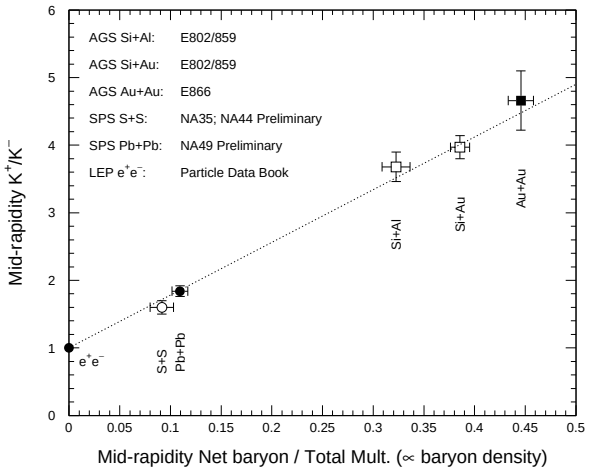

Figure 2: Mid-rapidity K^+/K^- ratio as function of the mid-rapidity ratio of net-baryon yield over total multiplicity in heavy ion collisions at the AGS and the SPS. Rapidity integrated K^+/K^- ratio in e^+e^- at LEP is also shown. The straight line is to guide the eye.

In Fig. 3, the total yield K^+/K^- ratios in heavy ion collisions are compared to those in N+N [40,41,42,43] at various bombarding energies. The ratio strongly depends on the bombarding energy in both heavy ion and N+N collisions.

However, the ratios are higher in heavy ion collisions than in N+N at the same energies. The dependence in N+N can be understood by the higher production threshold for K^- than K^+. The higher ratio in heavy ion collisions is qualitatively consistent with the following conjecture: each nucleon suffers multiple interactions in heavy ion collisions, where subsequent interactions happen at lower energy than the primary interaction, producing more K^+'s relative to K^-'s. The ratio of K^+/K^- in heavy ion collisions over that in N+N (referred as K^+/K^- enhancement) is shown in the insert of Fig. 3. The enhancement is higher in heavy system than in light system, which is consistent with the multiple collision picture. However, the enhancement seems independent of bombarding energy in systems with similar sizes.

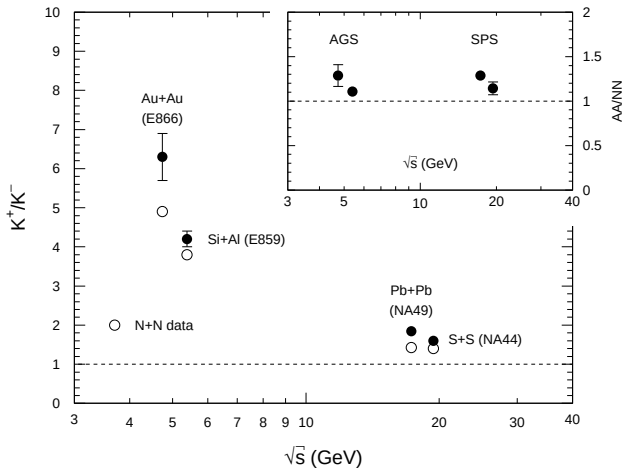

Figure 3: Total yield K^+/K^- ratio (except for Pb+Pb, the mid-rapidity ratio is used) as function of bombarding energy for N+N (open points) and heavy ion collisions (filled points). The ratios of K^+/K^- in heavy ion collisions over these in N+N are plotted in the insert.

3 Two-particle correlation functions

Two-particle correlation functions provide space-time information of the particles at freeze-out,[44,45] which cannot be obtained from single-particle distributions. Due to quantum interference, the probability to find two identical pions (bosons) with low momentum difference is enhanced. The width of the 2π correlation function after correction for Coulomb interaction is inversely related to the effective size of the pion source. Because of the correlation between space-time and momentum of the particles produced in heavy ion collisions

at freeze-out, due to the collision dynamics and collective behavior such as flow, particles within a limited momentum range are emitted from a limited space-time region of the source. The two-particle correlation function therefore measures, at small momentum difference, a limited region of the source.

NA49 has measured $2h^-$ correlation functions. [16] Based on a model incorporating both longitudinal and transverse flow, [46,47,48] the transverse and longitudinal radii were determined to be 6–8 fm at mid-rapidity, dropping by 2–3 fm to forward rapidity (Fig.4 in Ref. [16]). This size, compared to the 1-dimensional Gaussian radius $\sigma_{\rm Pb} \approx 3$ fm of the initial nuclei, implies that the collision system has gone through significant expansion before freeze-out. The radius parameters decrease with pair transverse momentum $p_\perp$ (Fig.6 in Ref. [16]). This behavior was also seen in S+A collisions [49,50], and is consistent with transverse radial flow. Combined with the single-particle transverse distributions, the freeze-out temperature (assumed to be the same for all particle species) and the transverse radial flow velocity at the source surface were estimated to be $T = 120 \pm 12$ MeV and $\beta_\perp = 0.55 \pm 0.12$, respectively.

Similar $p_\perp$ dependence of the correlation length has been found in Z^0 hadronic decays in e^+e^- annihilation at LEP. By including all final particles, the LUND model calculation reproduces the dependence. [51] The conjecture is that contribution from resonance decays, dominant at low $p_\perp$, enlarges the correlation length. The $p_\perp$ dependence of the correlation length in e^+e^- may also be due to space-time-momentum correlation arising from large formation time of high $p_\perp$ particles. Study of the effects of resonance decays and particle formation time on the source size measurement of heavy ion collisions, besides the effect of transverse radial flow, is underway. [52]

The baryon density plays an important role in the dynamical evolution of heavy ion collisions. [53,54] To measure baryon density, one needs information on the space-time extent of the baryon source, which is not necessarily the same as that of the pion's. The space-time extent of the baryon source at freeze-out can be measured by the two-proton correlation function. The two-proton correlation function has very different characteristics from the 2π correlation function. [44,55] Due to Fermi statistics, strong interaction between two protons is primarily due to 1/4 S-wave attractive interaction of the spin singlet and 3/4 P-wave repulsive interaction of the spin triplet. The combined strong and Coulomb interactions generate a peak in the two-proton correlation function at roughly $q_{\rm inv} = \sqrt{-q_\mu q^\mu}/2 \approx 20$ MeV/c, where $q_{\rm inv}$ is the momentum magnitude of either proton in the rest frame of the pair, and q_μ is the difference of the proton four-momentum vectors. The peak height above 1 is inversely proportional to the effective volume of the proton source.

While 2π correlation function measurements are common, measurements of

two-proton correlation functions are rare. NA49 has measured the two-proton correlation function at mid-rapidity. This is the first such measurement in Pb+Pb collisions at the SPS. The protons are mostly primordial nucleons, since baryon-antibaryon pair production contribution is at the level of 10% at SPS energy. [56,57] The measured two-proton correlation function is shown in Fig. 4. The peak at $q_{\rm inv} \approx 20$ MeV/c is evident and the height is 1.14 ± 0.04. The correlation function does not go to zero at $q_{\rm inv} = 0$ because of the contamination of protons from weak decays; there, the effect of the experimental momentum resolution is negligible. The deviation of the correlation function from 1 at large $q_{\rm inv}$ is currently under investigation.

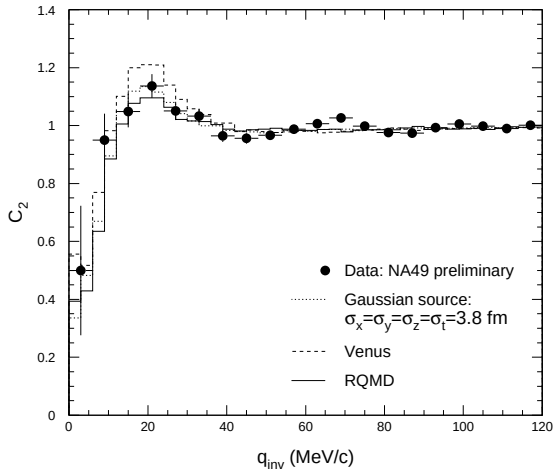

Figure 4: Two-proton correlation functions (not corrected for protons from weak decays) at mid-rapidity measured by NA49 (points), calculated for a Gaussian source (dotted histogram), and calculated for protons generated by RQMD (solid histogram) and by Venus (dashed histogram).

In order to interpret the proton freeze-out conditions, we employed the approach of comparing the measured two-proton correlation function with theoretical calculations. Given the proton phase space distribution, the two-proton correlation function was calculated using the Koonin-Pratt Formalism. [55,58] The experimental momentum resolution was included in the calculation. For the proton freeze-out distribution, we used two approaches. (I) Gaussian sources were generated with widths $\sigma_x = \sigma_y = \sigma_z = \sigma$ for the space coordinates and $\sigma_t = 0$ and σ for the time duration. The momentum was generated by a thermal distribution of temperature $T = 120$ MeV. The Gaussian sources do not have space-time-momentum correlation. (II) Protons were generated by two dynamical models, the Relativistic Quantum Molecular Dy-

namics (RQMD) model (v2.3) [59,60,61,62] and the Venus model (v4.12). [63] The protons have correlation between space-time and momentum intrinsic to the dynamical evolution of the models. The strength of the calculated correlation functions for (I) were reduced by 30% to account for the contamination of protons from weak decays. In the calculation for (II), the experimental acceptance was applied to the protons, and experimental effects in the accidental reconstruction of weak decay products as primary protons were incorporated.

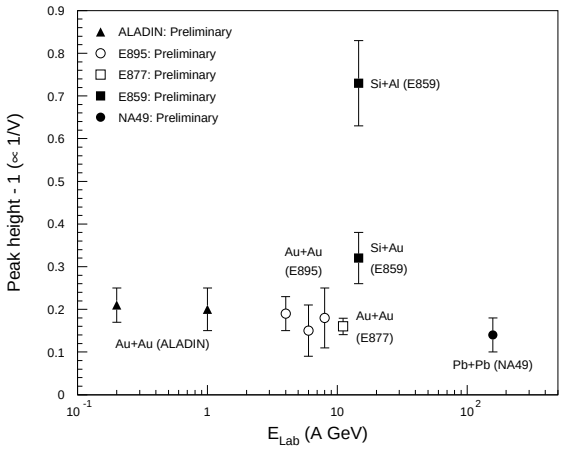

Figure 5: Peak height above 1 of measured two-proton correlation functions as function of beam energy. Contaminations of protons from weak decays are not corrected. The correction would bring up the Pb+Pb point by approximately 30%. The corrections are negligible for data at lower energies.

Comparison between the calculations and the experimental data showed that the Gaussian source with $\sigma_x = \sigma_y = \sigma_z = \sigma_t = 3.8$ fm well describes the data. The calculated correlation function is plotted in Fig. 4. We note that $\sigma = 3.8$ fm is slightly larger than the initial 1-dimensional nuclei size $\sigma_{\rm Pb} \approx 3$ fm, and is significantly smaller than the radius extracted from the $2h^-$ correlation function. The 1-dimensional effective size of the Gaussian source, calculated from the mean separation between protons in the pair rest frame, is $\sigma_\Delta/\sqrt{2} = 4.0$ fm. We have also studied Gaussian sources with extreme shapes: $\sigma_x = \sigma_y >> \sigma_z$ and $\sigma_x = \sigma_y << \sigma_z$ (both $\sigma_t = 0$). They cannot describe the data satisfactorily. The calculated two-proton correlation functions for RQMD and Venus are also shown in Fig. 4. Venus overpredicts the strength of the correlation function, while RQMD slightly underpredicts its strength. The mean separation between protons in the pair rest frame are $(\sigma_{\Delta x}, \sigma_{\Delta y}, \sigma_{\Delta z}) = (6.76, 5.34, 8.35)$ fm for RQMD, and $(4.41, 4.50, 5.44)$ fm for Venus, where z

is the longitudinal coordinate. The 1-dimensional effective size, $\sigma_\Delta/\sqrt{2} = \sqrt[3]{\sigma_{\Delta x}\sigma_{\Delta y}\sigma_{\Delta z}}/\sqrt{2}$, are 4.74 fm and 3.37 fm, respectively for RQMD and Venus. We note that no simple relation exists between $\sigma_\Delta/\sqrt{2}$ and the apparent single-proton source size in the models due to the dynamics.

We now comment on our two-proton correlation function measurement in the context of other measurements. The pion source volume is measured to be proportional to the pion multiplicity, [64,65,66] which increases steadily with beam energy in similar colliding systems. [67] Due to the large pion-nucleon cross-section, one would expect that protons and pions freeze-out under similar conditions, therefore, the proton source size would increase with beam energy as well. However, our measurement, in conjunction with preliminary results obtained at GSI [68,69] and AGS energies, [70] shows that the peak heights of the correlation functions in Au+Au and Pb+Pb collisions are rather insensitive to beam energy (Fig. 5). This means that the effective volumes of freeze-out protons are similar in these collisions over the wide energy range. More detailed studies are needed to understand the instrumental effects and the change in space-time-momentum correlation as function of the beam energy.

4 Conclusions

We conclude the following for central Pb+Pb collisions at the SPS:

- Strong baryon stopping. Baryon stopping in Pb+Pb central collisions is stronger than in S+S. The baryon spatial density achieved in Pb+Pb central collisions is higher than in S+S at the SPS, and is lower than in Au+Au at the AGS. The large baryon density resulted in a large K^+/K^- ratio. The enhancement in the ratio in heavy ion collisions of similar systems over N+N does not depend on the bombarding energy.
- Strong transverse radial flow. Inverse slopes of m_T distributions in the central rapidity region are larger in Pb+Pb central collisions than in S+S at the SPS and in Au+Au at the AGS. The radius parameters from $2h^-$ correlation function suggest strong expansion. The values of freeze-out temperature and transverse radial flow velocity are, however, model-dependent.
- Secondary particle rescattering in heavy ion collisions may be the driving force for the large baryon stopping, the strong transverse radial flow, and the K^+/K^- enhancement.
- No excessive entropy production. The negative hadron rapidity distribution scales with number of participants from S+S to Pb+Pb central collisions. No indication of excessive entropy production in Pb+Pb central collisions, compared to S+S, is found.

- Freeze-out source size. Effective size of the pion source extracted from the measured $2h^-$ correlation function is 6–8 fm at mid-rapidity. Effective size of the proton source extracted from the measured two-proton correlation function at mid-rapidity is 4 fm.

References

1. T. D. Lee and G. C. Wick. *Phys. Rev. D*, 9:2291, 1974.
2. J. Rafelski. *Phys. Rep.*, 88:331, 1982.
3. L. McLerran. *Rev. Mod. Phys.*, 58:1021, 1986.
4. B. Müller. *Nucl. Phys.*, A544:95c, 1992.
5. B. D. Keister and L. S. Kisslinger. *Phys. Lett. B*, 64:117, 1976.
6. *Nucl. Phys.*, A610, 1996, A638, 1998. QM'96 and QM'97 proceedings.
7. R. Koch, B. Müller, and J. Rafelski. *Phys. Rep.*, 142:167, 1986.
8. T. Matsui and H. Satz. *Phys. Lett. B*, 178:416, 1986.
9. E. V. Shuryak. *Phys. Lett. B*, 78:150, 1978.
10. X.-N. Wang and M. Gyulassy. *Phys. Rev. Lett.*, 68:1480, 1992.
11. M. Gyulassy, D. H. Rischke, and B. Zhang. *Nucl. Phys.*, A613:397, 1997.
12. H. Sorge *et al.* *Phys. Lett. B*, 271:37, 1991.
13. R. Mattiello *et al.* *Phys. Rev. Lett.*, 63:1459, 1989.
14. T. Alber *et al.* (NA49 Coll.). *Phys. Rev. Lett.*, 75:3814, 1995.
15. H. Appelshauser *et al.* (NA49 Coll.). nucl-ex/9810014.
16. H. Appelshauser *et al.* (NA49 Coll.). *Eur. Phys. J.*, C2:661, 1998.
17. H. Appelshauser *et al.* (NA49 Coll.). In preparation.
18. C. Bormann *et al.* (NA49 Coll.). *J. Phys.*, G23:1817, 1997.
19. H. Appelshauser *et al.* (NA49 Coll.). *Phys. Lett. B.* in press, nucl-ex/9810005.
20. H. Appelshauser *et al.* (NA49 Coll.). *Phys. Rev. Lett.*, 80:4136, 1998.
21. S. Wenig *et al.* *Nucl. Instr. and Meth.*, A409:100, 1998.
22. B. Lasiuk *et al.* *Nucl. Instr. and Meth.*, A409:402, 1998.
23. F. Puehlhofer (NA49 Coll.). *Nucl. Phys.*, A638, 1998.
24. H. Appelshauser *et al.* (NA49 Coll.). *Eur. Phys. J.*, A2:383, 1998.
25. L. Ahle *et al.* (E802 Coll.). *Phys. Rev. C*, 57:R466, 1998.
26. T. Alber *et al.* (NA35 Coll.). *Eur. Phys. J.*, C2:643, 1998.
27. J. Bachler *et al.* (NA35 Coll.). *Phys. Rev. Lett.*, 72:1419, 1994.
28. J. Bachler *et al.* (NA35 Coll.). *Heavy Ion Physics*, 4:71, 1996.
29. M. Aguilar-Benitez *et al.* *Z. Phys. C*, 50:405, 1991.
30. G. Roland (NA49 Collaboration). *Nucl. Phys.*, A638:91, 1998.
31. I. G. Bearden *et al.* (NA44 Coll.). *Phys. Rev. Lett.*, 78:2080, 1997.
32. F. Wang. PhD thesis, Columbia University, 1996.

33. T. Abbott *et al.* (E802 Coll.). *Phys. Rev. C*, 50:1024, 1994.
34. D. P. Morrison. PhD thesis, MIT, May 1994.
35. B. A. Cole (E802 Coll.). *Nucl. Phys.*, A590:179c, 1995.
36. L. Ahle *et al.* (E802 Coll.). *Phys. Rev. C*. In press.
37. F. Wang (E802 Coll.). In *Proceedings of Heavy-Ion Physics at the AGS (HIPAGS'96)*. Wayne State University, WSU-NP-96-16, 1996.
38. H. Bøggild *et al.* (NA44 Coll.). 1998. nucl-ex/9808002.
39. Particle Data Group. *Eur. Phys. J.*, C3:201, 1998.
40. M. Gazdzicki and O. Hansen. *Nucl. Phys.*, A528:754, 1991.
41. H. Fesefeldt *et al. Nucl. Phys.*, B147:317, 1979.
42. V. Blobel *et al. Nucl. Phys.*, B69:454, 1974.
43. E. Albini *et al. Nucl. Phys.*, B84:269, 1975.
44. D. H. Boal *et al. Rev. Mod. Phys.*, 62:553, 1990.
45. G. Baym. *Acta Phys. Polon.*, B29:1839, 1998.
46. U. Heinz *et al. Phys. Lett.*, B382:181, 1996.
47. S. Chapman, J. R. Nix, and U. Heinz. *Phys. Rev. C*, 52:2694, 1995.
48. U. Heinz. *Nucl. Phys.*, A610:264c, 1996.
49. T. Alber *et al.* (NA35 Coll.). *Z. Phys. C*, 66:77, 1995.
50. H. Beker *et al.* (NA44 Coll.). *Phys. Rev. Lett.*, 74:3340, 1995.
51. B. Andersson and M. Ringner. *Nucl. Phys.*, B513:627–644, 1998.
52. F. Wang, S. Esumi, and N. Xu. In preparation.
53. P. Koch, J. Rafelski, and W. Greiner. *Phys. Lett. B*, 123:151, 1983.
54. K. S. Lee *et al. Phys. Rev. C*, 37:1452, 1988.
55. S. E. Koonin. *Phys. Lett.*, 70B:43, 1977.
56. T. Alber *et al.* (NA35 Coll.). *Phys. Lett. B*, 366:56, 1996.
57. I. G. Bearden *et al.* (NA44 Coll.). *Phys. Rev. C*, 57:837, 1998.
58. S. Pratt and M. B. Tsang. *Phys. Rev. C*, 36:2390, 1987.
59. H. Sorge, H. Stocker, and W. Greiner. Annals of Physics, 192:266, 1989.
60. H. Sorge *et al. Phys. Lett. B*, 289:6, 1992.
61. H. Sorge. *Nucl. Phys.*, A498:567c, 1989.
62. H. Sorge. *Phys. Rev. C*, 52:3291, 1995.
63. K. Werner. *Phys. Rep.*, 232:87, 1993.
64. I. G. Bearden *et al.* (NA44 Coll.). *Phys. Rev. C*, 58:1656, 1998.
65. I. G. Bearden *et al.* (NA44 Coll.). *Z. Phys. C*, 75:619, 1997.
66. M. D. Baker (E802 Coll.). *Nucl. Phys.*, A610:213c, 1996.
67. M. Gazdzicki and D. Roehrich. *Z. Phys. C*, 65:215, 1995.
68. C. Schwarz *et al.* (ALADIN Coll.). nucl-ex/9704001.
69. R. Fritz *et al.* (ALADIN Coll.). nucl-ex/9704002.
70. S. Panitkin *et al.* (E895 Coll.). E895 preliminary.